EUROPHYSICS LETTERS 10 February 1996

Europhys. Lett., **33** (5), pp. 371-376 (1996)

On the nature of shear thinning in nanoscopically confined films

E. MANIAS[1], I. BITSANIS[2], G. HADZIIOANNOU[3] and G. TEN BRINKE[3]

[1] *Materials Science & Engineering, Cornell University*
Bard Hall, Ithaca NY 14583, USA
[2] *Chemical Engineering, University of Florida - Gainesville, FL 32611, USA*
[3] *Polymer Science Laboratory and Materials Science Centre, University of Groningen*
Nijenborgh 4, 9747 AG Groningen, The Netherlands

(received 19 September 1995; accepted in final form 21 December 1995)

PACS. 68.15+e – Liquid thin films.
PACS. 66.20+d – Diffusive momentum transport (including viscosity of liquids).
PACS. 83.10Ji – Fluid dynamics (nonlinear fluids).

Abstract. – Non-Equilibrium Molecular Dynamics (NEMD) computer simulations were employed to study films in nanometer confinements under shear. Focusing on the response of the viscosity, we found that nearly all the shear thinning takes place inside the solid-oligomer interface and that the adsorbed layers are more viscous than the middle part of the films. Moreover, the shear thinning inside the interfacial area is determined by the wall affinity and is largely insensitive to changes of the film thickness and the molecular architecture. The rheological response of the whole film is the weighted average of these two regions —"viscous" interfacial layer and bulk-like middle part— resulting in *an absence of a universal response* in the shear thinning regime, in agreement with recent SFA experiments of fluid lubricants.

Recent experimental studies of ultra-thin films by the Surface Forces Apparatus (SFA) reveal striking behaviour in the rheological response of lubricating films when confined in dimensions comparable to the molecular size [1]-[10]. Such films become strongly inhomogeneous [5] and their effective viscosity increases dramatically when reducing the film thickness [2]. Moreover, they exhibit shear thinning for very moderate shear rates and the onset of this non-Newtonian behaviour shifts to lower shear rates in narrower confinements [6], [7]. Molecular-Dynamics (MD) computer simulations have proven to be effective in interpreting this counter-intuitive behaviour of nanoscopically confined films [11]-[15] and unveiled the *origin of the "glassy" dynamics* in ultra-thin confinements [11], [12].

On the other hand, the phenomenon of shear thinning in *nano*-confinements is not well understood. Pioneering shear-SFA studies of oligomers demonstrated that, in the non-Newtonian regime, the *effective* viscosity seemed to follow a universal behaviour: $\eta_{\text{eff}} \sim \dot{\gamma}^{-2/3}$ [6]. Subsequent non-equilibrium MD simulations verified this power law, but at the same time showed the possibility of a richer response to shear [15]. Since then, a variety of shear thinning power laws have been reported in the literature [6],[7],[4]. In all these cases a common behaviour is observed for wide enough films: linear Newtonian-like response for small shear rates, followed by extensive, power law, shear thinning.

In order to gain more insight in the mechanisms of shear thinning in films of nanometer thickness, we carried out MD simulations of confined oligomer fluids under Couette flow [12]-[14]. A well-studied bead-spring model chain [11]-[16] is confined between two atomically

TABLE I. – *Power law fits* ($\eta_{\text{eff}} \sim \dot{\gamma}^{-\alpha}$) *to the shear thinning regions for various systems. Nearly all the shear thinning takes place inside the solid-oligomer interface and the power law —describing the response of viscosity in this region— is determined by the wall affinity, whereas it is rather insensitive to the oligomer molecule architectures. In the middle of the film we only fit a power law for comparison reasons, inspired by the experimental standard procedures (within parenthenses the fit-uncertainty of the last decimal).*

Local effective viscosities				
wall affinity $\epsilon_{\text{w}}(\epsilon)$	pore width $h(\sigma)$	type of oligomer	α middle part	α first layer
1.0	6.0	linear decamer	0.30(1)	0.38(1)
1.0	6.0	linear hexamer	0.26(4)	0.40(2)
1.0	6.0	branched 6mer	0.19(3)	0.44(3)
1.0	6.0	3arm star 7mer	0.20(1)	0.42(3)
1.0	7.0	linear hexamer	0.18(2)	0.41(2)
1.0	7.0	branched 6mer	0.12(3)	0.43(3)
1.0	10.0	linear pentamer	0.16(2)	0.44(2)
1.5	10.0	linear pentamer	0.16(2)	0.53(3)
2.0	10.0	linear pentamer	0.16(2)	0.69(2)
2.0	6.0	linear hexamer	0.13(2)	0.62(5)
3.0	10.0	linear pentamer	0.16(2)	~ 0.80
3.0	6.0	linear hexamer	0.14(1)	~ 0.78

structured surfaces. The details of the simulation method and systems are described elsewhere [11]-[14]. The interchain interactions in this model are repulsive, whereas the wall-fluid interactions are simulated via a Lennard-Jones potential, with an ϵ_{w} LJ energy parameter. ϵ_{w} corresponds to the solid-atom–chain-segment excess adhesive energy and thus determines the strength of the fluid adsorption on the solid wall [11], [14]. Several different oligomer molecules were studied (table I).

In order to determine the actual shear rate that the film undergoes, one has to take into account the flow boundary conditions at the wall and the slip. For $\epsilon_{\text{w}} = 1.0\epsilon$, there is slip between the wall and the fluid, whereas for stronger wall affinities the slip is located inside the fluid film between the adsorbed layer and the rest of the system (fig. 1) [13]. When calculating the induced shear rate across the whole film the slip is subtracted. Moreover, a local shear rate at z_0 can be defined as $\dot{\gamma}_{\text{local}} = \left(\frac{\partial v_x}{\partial z}\right)_{z_0}$. Although for these strongly inhomogeneous systems the definition of viscosity is subtle, a quantity that is correlated with the resistance of the fluid to flow is usually defined by the mean frictional force per unit area (which, in our case, is the xz stress component) divided by the induced shear rate [15]: $\eta_{\text{eff}} = (\tau_{xz}/\dot{\gamma}) = (F_{\text{frict}}/S\,\dot{\gamma})$. This quantity has dimensions of viscosity —this is also the way that η_{eff} is measured in SFA experiments [1]-[4], [6]-[8]— and is named *effective* viscosity; it characterizes the response of the whole film. A *local effective viscosity* can also be defined as the τ_{xz} stress divided by the local shear rate. From the steady-state velocity profiles developed across these films (fig. 1) it becomes obvious that the local shear rate inside the adsorbed layer is smaller than in the middle and thus the fluid in the vicinity of the wall is "more viscous" than further away from the surfaces. The development of such inhomogeneous velocity profiles is discussed in detail elsewhere [13], [15].

In fig. 2 the dependence of the *total film effective viscosity* on the shear rate is shown for two film thicknesses. In agreement with experiments, a decrease in the film width causes an increase of the effective viscosity and the onset of the shear thinning shifts to smaller shear

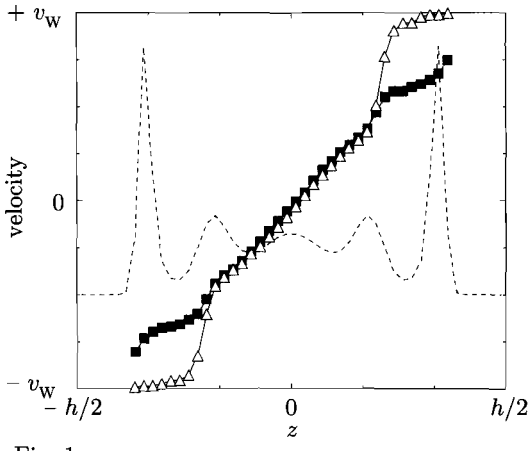

Fig. 1.

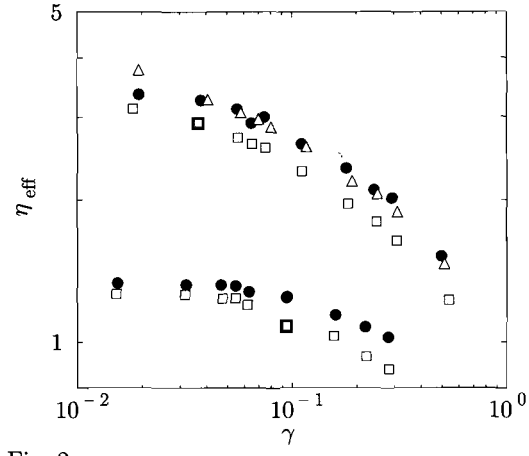

Fig. 2.

Fig. 1. – Density (– – –) and steady-state velocity profiles for a fluid oligomer lubricant confined between weakly (■ $\epsilon_w = 1$) and strongly (△ $\epsilon_w = 2$) adsorbing surfaces ($h = 6\sigma$). A sufficiently high wall velocity (v_w) is presented for slip to appear near the surfaces ($\epsilon_w = 1$) or inside the film ($\epsilon_w = 2$).

Fig. 2. – Total film effective viscosity *vs.* shear rate, for different molecular architectures (□ linear hexamers, • branched hexamers and △ star heptamers) and for films with $h = 7$ (bottom) and $h = 6$ (top).

rates for narrower films. The absolute value of η_{eff} is not very important as it depends strongly on pressure —and so on density— ([15], fig.2 *b*) and so does the onset of shear thinning. The effect of pressure on the effective viscosity is observed in SFA experiments: for small oligomers a strong exponential increase is reported [7], and also in realistic MD simulations of alkanes [17]. For these reasons the viscosities presented in fig. 2 are normalized by the viscosity of a bulk with the same density as the middle part of the film. Moreover, we chose to work at such pressures that the viscosities in the middle of the pore are near their bulk value.

Keeping in mind that the strong confinement of our films results in a highly inhomogeneous system —characterized by both density oscillations and regions of different viscosity— the really interesting quantity is the local η_{eff}. A typical response to shear of a confined film is shown in fig. 3 *a*). Although inside the solid-oligomer interface the fluid exhibits strong shear thinning, the middle part of the film behaves almost as a Newtonian fluid, *i.e.* nearly all the shear thinning takes place inside the adsorbed first layer. Furthermore, as expected from the velocity profile (△ in fig. 1), the viscosity inside the first layer is higher than in the middle part. At the same time, the viscosity in the middle is only slightly higher than the bulk value. This strong local variation of the effective viscosity was long suspected by experimentalists [8], [2] and even proposed as an explanation for their observations —both in equilibrium [8] and shearing [7]— but herein is clearly demonstrated. Finally, the response of the total film is the *average* of the response inside the first layer and in the middle of the system *weighted* by the fraction of the system in these two regions ([1]).

For the $h = 6\sigma, \epsilon_w = 1\epsilon$ films, the power law decrease of this η_{eff} in the shear thinning region *across the whole film* is a $\eta_{eff} \sim \dot{\gamma}^{-1/2}$ (fig. 2), this dependence coincides with SFA experiments of wide enough films [4]-[7] and constant-volume NEMD simulations of flow in the bulk [17]-[19] and under confinement [15], but not with constant-pressure MD simulations [15] which find $\eta \sim \dot{\gamma}^{-2/3}$. Recent NEMD studies comparing constant-volume and constant-pressure simulations [20] also find this deviation in the exponents for bulk oligomers. Under

([1]) This we calculated to be valid for all the systems, and is a natural consequence of a fluid with viscosity inhomogeneities subjected to flow.

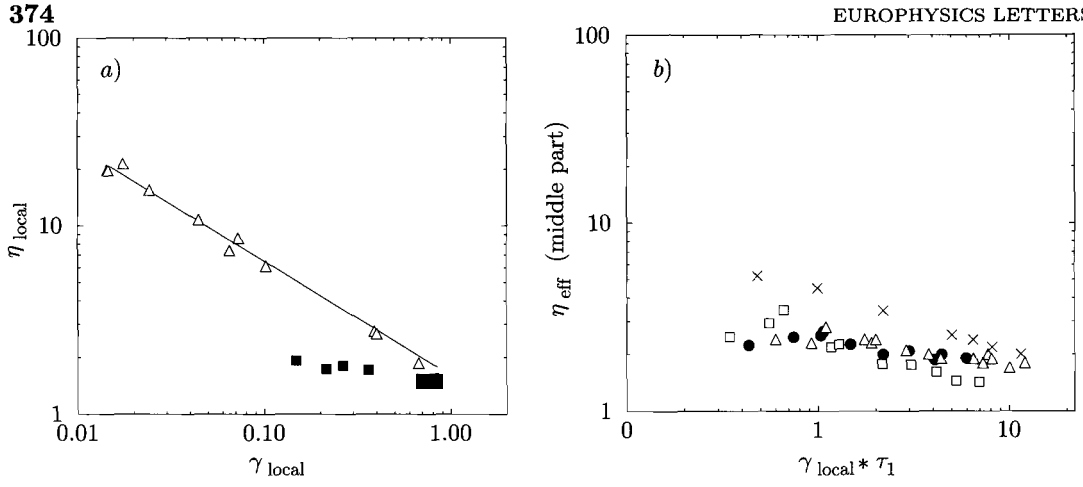

Fig. 3. – *a) Local* effective viscosity *vs.* shear rate inside the *first layer* (△) and in the middle part (■) of the film (hexamers, $h = 6$, $\epsilon_w = 2$). Almost all shear thinning takes place inside the solid-oligomer interface. *b) Local* effective viscosity *vs.* shear rate *in the middle part of the films* (• branched hexamer ($h = 6$), □ linear hexamer ($h = 6$), △ linear pentamer ($h = 10$) and × decamer ($h = 6$)). In order to compare, all viscosities are scaled with the viscosity of the corresponding bulk system (bulk with the same density, pressure and molecular architecture).

the same pressure and wall affinity the effect of the molecular architecture on the response of the total film effective viscosity is found to be minor, in agreement with previous computer simulations [17],[19],[21] and contrary to what is expected from shear thinning in the bulk [22] and from SFA experiments of much longer polymers [3].

In fig. 3*b*) the behaviour *in the middle of the pore* is presented. There is only a weak shear thinning in this region for our short oligomers. The pore hosting the pentamers is wide enough ($h = 10$) to guarantee that the middle part of the system is sufficiently far from the surfaces; for the rest of the systems narrower confinements ($h = 6$) are used in order to see the effects of stronger geometric constraints. In this middle part, the non-Newtonian character is more pronounced for the longer coils —decamers shear-thin more than hexamers and these more than pentamers (table I)— and also for the linear hexamers compared to the branched ones. This is exactly what is expected to happen in the bulk [22], *i.e.* the shear thinning is expected to start at lower shear rates for long linear unentangled chains than for shorter ones or for branched chains of the same size.

Most of the experiments reporting power laws for shear thinning are studying films only a few molecular diameters wide, which implies that they are probing mainly the effective viscosity inside the first layer. In this respect, a more relevant quantity is the *local effective viscosity inside the solid-oligomer interface,* presented in fig. 4. In fig. 4*a*) wide films of pentamers are used in order for the two interfacial regions to be well separated and a variety of wall affinities have been simulated. It becomes clear that the response of the oligomers to shear is determined by the wall affinity (table I). For weakly adsorbing surfaces ($\epsilon_w = 1$) the systems exhibit a Newtonian-like behaviour for the lower shear rates, with η_{eff} being independent of $\dot{\gamma}$, but for stronger adsorption energies the systems shear-thin throughout the range of shear rates employed in our simulations. The use of a $\eta_{eff} \sim \dot{\gamma}_{local}^{-\alpha}$ power law to describe the shear thinning region inside the first layer seems to be justified and there is a systematic increase in the exponent with ϵ_w (table I). Namely, α is -0.44 in the linear part for $\epsilon_w = 1.0$ and becomes -0.53 for $\epsilon_w = 1.5$ and -0.69 for $\epsilon_w = 2.0$. For stronger wall affinity ($\epsilon_w = 3$) it is very difficult for the slope of the velocity profile to be measured accurately inside the solid-oligomer interface [13] and conclusions can be drawn from strong flows only; α in this case is approximately -0.78. For our linear hexamers the same power laws are valid (table I) and the exponents are -0.40 for $\epsilon_w = 1.0$ (fig. 4*b*)), -0.62 for $\epsilon_w = 2.0$ (fig. 3*a*)) and ~ -0.8 for $\epsilon_w = 3$. In fig. 4*b*)

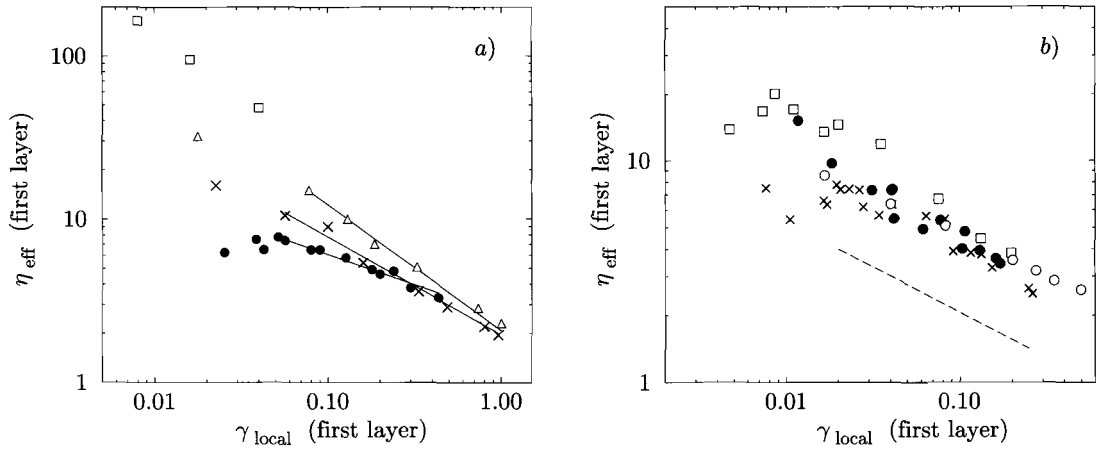

Fig. 4. – *Local* effective viscosity *vs.* shear rate *inside the solid-oligomer interface. a)* the dependence on wall energetics: systems of pentamers in *wide* enough pores ($h = 10$) to allow the development of two well-separated, independent interfacial layers. For higher shear, rates the shear thinning can be clearly described by a power law which is determined by the wall energetics (ϵ_w). The fitted straight lines are shown over the fitted range of γ and the exponents are given in table I (for $\epsilon_w = 1.0$, 1.5 and 2.0 the power law exponent is $\alpha = 0.44$, 0.53 and 0.69, respectively) (• $\epsilon_w = 1.0$, × $\epsilon_w = 1.5$, △ $\epsilon_w = 2.0$, □ $\epsilon_w = 3.0$). *b)* the dependence on molecular architecture: systems in *thin* pores ($h = 6$) confined between weakly physisorbing surfaces ($\epsilon_w = 1$); there is a weak only dependence of the shear thinning power law on the molecule architecture; the dashed line follows a $\eta^{-0.41}$ power law over the shortest γ-range used for the fits (□ linear hexamer, × branched hexamer, • star heptamer and ○ linear decamer).

the local η_{eff} in the interfacial layer is plotted against the local shear rate for a variety of molecules confined in narrower pores ($h = 6$). For these flexible model chains the power law shear thinning inside the solid-oligomer interface does not depend markedly on the molecule architecture (table I). Furthermore, the effective viscosity is almost an order of magnitude higher than in the middle of the same film and increases with stronger wall attractions.

Our previous studies [12]-[14] revealed a strong tendency of the adsorbed chains to align and stretch against the confining surface for the shear rates employed. This behaviour clearly is a major contribution to the shear thinning observed [22]. But, beyond this molecular alignment and deformation, other effects are expected to contribute for these flexible molecules as well, thus various intra- and inter-molecular mechanisms are brought into effect at different shear rates, and give rise to a variety of regimes with different viscosity dependences on shear rate[23].

Hence, by NEMD simulations of nanoscopically confined films under shear, we observed that the viscosity inside the solid-oligomer interface is increased compared to the bulk value, as expected by the dramatic increase of the relaxation times [11] and the simultaneous decrease of the transport coefficients therein [12]. The main findings are that nearly all the shear thinning takes place in exactly this region and that the power law —describing the response of viscosity in this region— is determined by the wall affinity, whereas it is rather insensitive to the oligomer molecular architectures. The behaviour of the whole film is the weighted average of the viscosities inside the interfacial layers and the middle part, which explains the absence of a universal law for the shear response of nanoconfined fluid lubricants. Consequently, the total viscosity is expected to scale as $\eta_{\text{eff}} \sim 1/h$, as observed for confined oligomers ([9] fig. 3).

The next question is how all these compare to the experimental observations. Although our simulations are under constant volume and the experiments are carried out under constant pressure, during the experiments the mica separation (wall-to-wall distance) is monitored and does not change much while shearing [6], [7]. The viscosity increases reported here are not as high as in some experiments [6], but one has to take into account that the loads used in

those experiments are much greater than the ones used by us, and the viscosity is expected to increase drastically with pressure [15], [7]. Moreover, the $\eta_{\text{eff}} \sim \dot{\gamma}^{-2/3}$ behaviour was obtained for small-ring silicones (octa-methyl-cyclo-tetra-siloxane: OMCTS) confined between mica in *ultra*-thin films of two ([6] fig. 2) or three ([7] fig. 6) confined layers, thus practically *only* the adsorbed layers are probed (it should be pointed out that the affinity between mica and siloxanes is very strong [9]). The same power law $\eta_{\text{eff}} \sim \dot{\gamma}^{-0.67}$ was observed for short n-alkanes (dodecane) under high pressures (120 kPa at $h \simeq 6\sigma$) ([6] fig. 2), whereas for dodecane under much smaller pressures (6.5 Pa at $h \simeq 6.5\sigma$) $\eta_{\text{eff}} \sim \dot{\gamma}^{-0.52}$ was obtained ([7] fig. 3) with a simultaneous threefold decrease of viscosity compared to [6]. Fluids of smaller affinity for mica (PPMS) exhibit shear thinning following $\eta_{\text{eff}} \sim \dot{\gamma}^{-0.44}$ for $h = 6$ and 5σ ([4] fig. 5*a*), and behave as Newtonian fluids in wide films of $h \simeq 17\sigma$ ([4] fig. 5*a*). When weakly adsorbing surfaces are used (OTE-covered mica) "*the viscosity drops below the limit for experimental measurement*" ([10], p. 3878). Finally, NPT non-equilibrium MD simulations of oligomer films under shear [15] showed a $\eta_{\text{eff}} \sim \dot{\gamma}^{-2/3}$ shear thinning power law, which fits best the response of ultra-thin films of two layers and wider films under high pressures ([15], fig. 2 and 3). The same simulations under constant volume (NVT) gave a slower decrease: $\eta_{\text{eff}} \sim \dot{\gamma}^{-1/2}$.

In summary, MD simulations revealed that in sheared nanoconfined oligomer films the viscosity inside the solid-oligomer interface is much higher than in the middle of the film (and increases with surface affinity). Moreover, nearly all the shear thinning takes place inside this adsorbed layer, whereas the response of the whole film is the weighted average of the viscosity in the middle and inside the interface. Finally, there was found not to exist any universal power law describing shear thinning —in agreement with SFA experiments— but the power is determined by the wall energetics and is insensitive to molecular architecture.

REFERENCES

[1] GEE M. L., MCGUIGGAN P. M., ISRAELACHVILI J. N. and HOMOLA A. M., *J. Chem. Phys.*, **93** (1990) 1895.
[2] GRANICK S., *Science*, **253** (1991) 1374.
[3] HOMOLA A. M., NGUYGEN H. V. and HADZIIOANNOU G., *J. Chem. Phys.*, **94** (1991) 2346.
[4] GRANICK S., HU H. and CARSON G. A., *Langmuir*, **10** (1994) 3867.
[5] CHAN D. Y. C. and HORN R. G., *J. Chem. Phys.*, **83** (1985) 5311.
[6] HU H., CARSON G. A. and GRANICK S., *Phys. Rev. Lett.*, **66** (1991) 2758.
[7] CARSON G., HU H. and GRANICK S., *Tribol. Trans.*, **35** (1992) 405.
[8] MONTFORT J. P. and HADZIIOANNOU G., *J. Chem. Phys.*, **88** (1988) 7187.
[9] VAN ALSTEN J. and GRANICK S., *Macromolecules*, **23** (1990) 4856.
[10] PEANASKY J., CAI L., GRANICK S. and KESSEL C., *Langmuir*, **10** (1994) 3874.
[11] BITSANIS I. and PAN C., *J. Chem. Phys.*, **99** (1993) 5520.
[12] MANIAS E., SUBBOTIN A., HADZIIOANNOU G. and TEN BRINKE G., *Mol. Phys.*, **85** (1995) 1017.
[13] MANIAS E., HADZIIOANNOU G., BITSANIS I. and TEN BRINKE G., *Europhys. Lett.*, **24** (1993) 99.
[14] MANIAS E., HADZIIOANNOU G. and TEN BRINKE G., *J. Chem. Phys.*, **101** (1994) 1721.
[15] THOMPSON P. A., GREST G. S. and ROBBINS M. O., *Phys. Rev. Let.*, **68** (1992) 3448; *Israel J. Chem.*, **35** (1995) 93.
[16] KREMER K. and GREST G., *J. Chem. Phys.*, **92** (1990) 5057.
[17] ROWLEY R. L. and ELY J. F., *Mol. Simul.*, **7** (1991) 303.
[18] EDBERG R., MORRISS G. P. and EVANS D. J., *J. Chem. Phys.*, **86** (1986) 4555.
[19] DAIVIS P. J., EVANS D. J. and MORRISS G. P., *J. Chem. Phys.*, **97** (1992) 616.
[20] DAIVIS P. J. and EVANS D. J., *J. Chem. Phys.*, **100** (1994) 541.
[21] PADILLA P. and TOXVAERD S., *J. Chem. Phys.*, **101** (1994) 1490.
[22] FERRY J. D., *Viscoelastic Properties of Polymers*, (John Wiley) 1980.
[23] SUBBOTIN A., SEMENOV A., MANIAS E., HADZIIOANNOU G. and TEN BRINKE G., *Macromolecules*, **28** (1995) 1511; **28** (1995) 3898; **28** (1995) 3901.